Comparison of methodologies for induction motor design

Devon D. S. Kibby

Master of Engineering

Department of Computer and Electrical Engineering

McGill University

Montreal, Quebec

July 2013

A thesis submitted to McGill University in partial fulfillment of the requirements of the degree of Master of Engineering

ACKNOWLEDGEMENTS

I would like to thank my supervisor, Prof. David Lowther, for giving me the invaluable gift of his time, as well as, his intellectual and financial support that enabled me to attend and complete my studies at McGill. Discussing all the research in this thesis with someone as knowledgeable and experienced in the field as Prof. Lowther has truly been an honor.

Secondly, I would like to thank all my friends and family, in Montreal and abroad, for their support and encouragement.

ABSTRACT

In the last few decades, the world of electric machine design, specifically induction machine design, has been reinvigorated by the introduction of power electronics. Where designers were once limited to a single alternating current waveform with constant voltage and frequency, power electronics have thrown all those assumptions out the window. The change has necessitated new design methods that go beyond the typical induction motor electrical equivalent circuit seen in every textbook for the last century and have sent designers back to first principles.

With that sentiment, early induction motor invention and improvements are explored. It is shown that even though the development and commercialization of the induction motor was quite rapid, the theory and understanding of the underlying physics kept pace. Basic design methodologies and tools, including the Hopkinson magnetic circuit and the Steinmetz equivalent circuit, from the so-called “'Golden Age' of induction motor development” are traced forward through textbook examples to support the claim.

Newer electric machine analyses are presented in the form of the modern treatment of the magnetic equivalent circuit, MEC, and the finite element method, FEM. A derivation of the MEC element from the magnetic scalar potential is completed utilizing the theory of tubes and slices to give a more tangible justification to the field assumptions made. The knowledge from these assumptions is then applied to the FEM to show how to construct an MEC element using the FEM. Tellegen's theorem is applied to the MEC and a brief

example given showing how one might compute the first-order sensitivity of a small change in stator windings in an induction motor to a small change in torque.

A brief overview of the engineering design process is described with a focus on augmentation with computer aided design tools, CAD. The equivalence shown between the MEC and FEM is used to support the idea that a FEM-based electric machine CAD package could be modified to utilize MEC assumptions or knowledge in order to reduce computation time when coarser models are favored, such as in the early design stages.

ABRÉGÉ

Depuis les dernières quelques décennies, l'industrie de la conception de la machine électrique, spécifiquement la conception de moteur à induction, a été revigoré par l'introduction des électroniques de puissance. Là ou les concepteurs étaient jadis limités à un courant alternatif avec fréquence et voltage constant, l'électronique de puissance est venue compliquer les lignes directrices de la conception. Ces changements ont nécessité des nouvelle méthodes qui vont au-delà du circuit équivalent typique mentionné dans tous les livres de référence depuis le dernier siècle et ont reporté les concepteurs aux principes de base.

C'est à partir de cette complication que l'évolution du moteur à induction depuis son invention est revisitée. Il a été démontré que, malgré son développement et sa commercialisation notablement rapides, la théorie du moteur à induction et notre compréhension des principes physiques ont suivi le rythme. Les méthodologies de base et outils de conception provenant du soi-disant âge d'or du moteur à induction, notamment le circuit magnétique Hopkins et le circuit équivalent Steinmetz, sont retracés dans les exemples à travers les livres de référence pour supporter la thèse.

L'analyse des machines électriques actuelles est présentée sous la forme du circuit magnétique équivalent (MEC) moderne et par le calcul par éléments finis (FEM). Une dérivation du MEC à partir du potentiel magnétique vectoriel est réalisée en utilisant la théorie des tubes et tranches pour justifier les hypothèses concernant les champs

électromagnétiques. Par la suite, ces hypothèses sont appliquées au calcul FEM pour démontrer la création d'un MEC à partir du calcul FEM. Le théorème de Tellegen est appliqué au MEC et un exemple concret est élaboré pour démontrer comment calculer la sensibilité de premier ordre entre un petit changement dans le bobinage électrique du stator et un petit changement dans le couple.

Un bref aperçu du procédé de conception est apporté avec un focus sur la contribution des logiciels de conception assistée par ordinateur (CAD). L'équivalence démontrée entre la méthode du MEC et celle par le calcul FEM est utilisée pour soutenir l'idée que les logiciels CAD basés sur le calcul FEM pourraient être modifiés pour inclure les hypothèses apportées par le MEC dans le but d'économiser le temps de calcul lorsque, durant les étapes préliminaires de la conception, un modèle simple suffirait.

TABLE OF CONTENTS

LIST OF FIGURES

CHAPTER 1
Introduction

``The scientist merely explores
that which exists,
while the engineer creates
what has never existed before."

Theodore von Kármán [1]

The process by which an engineer creates that which "has never existed before" is termed engineering design. Design, by definition, is the process of conception by imagination. The nothingness from which these designs, ideas, and plans spring remains implied and unmentioned; enigmas of the mind. Many of these ideas grow out of necessity to create useful machines, working to cleverly harness the natural phenomena of the universe.

The design process aims to solve a problem that is inherently poorly posed, incomplete, and to which no feasible solution may exist. Reducing failure in the search for solutions has captured the attention of many who study and work to improve the engineering design process itself. The critiquing, cataloging, and subdivision of the engineering design process has yielded an abundance of terms to describe and identify occurrences in a general design process; from the novelty of a design problem to selecting the best suited design methodology to describing a design stage and its proximity to a final solution, a reader will undoubtedly find a plethora of information in literature [2], [3].

One end result of such detailed breakdowns and descriptions is the creation of targeted tools specialized for specific types of problems and specific stages in the design process. They provide a resource to aid the designer in more effectively navigating the solution search space. The assistance provided can help to lower the level of domain experience needed, save time for known problems by using standardized design methodologies , and hopefully find a better solution more quickly than might otherwise be realizable.

In the modern age many new aids have presented themselves in the form of computer aided design, CAD, tools. These supports utilize the power of computers to perform modern mathematical analysis and graphical visualization in order to augment, reduce, or even fundamentally refocus portions of the design process. In many cases, what once could only be realized by expensive experiments and multiple physical design verifications, is now replaced by virtual experiments until the designer is sure the solution meets their requirements.

The ability of computers to perform flawless arithmetic calculations at incredible speed has fueled the rise of computational methods to power these CAD tools, such as: the finite difference method, the finite element method, and the boundary element method. The use of these computational methods highlights a shift to a design methodology that works directly from first principles rather than empirical results or previous work. While working from first principles might not be faster than previously popular methods, it allows the designer to explore a larger search space, encompassing more design candidates. With the ever increasing demand for more efficient, better performing, and smaller devices, designers are slowly embracing the use of CAD tools as previous methods have begun to show their limitations.

To find out where old methods are failing, first a little more has to be understood about the overall process. A cursory study of many successful design processes reveals a highly iterative structure. When designers find a solution to a problem, the success is remembered. Later, when a designer is presented with a problem that the designer perceives to be similar, knowledge of the previous success is translated to a new possible solution. The acute reader might call this strategy, "learning." By relying on previous solutions it is highly unlikely for the new solution to fail categorically. In the same vein, learning from the failed new solution and refining it in a second attempt, is a popular way to try again. The refinements or iterations then continue until successful or time runs out or the budget is exceeded.

While the aforementioned method, referred to in literature as a type of "case-based reasoning" [4], [5], is a tried and true method; it along with simplified analytical methods are no longer generating as many reliably successful solutions when faced with demanding modern design criteria because modern solutions can not always be found in the previous cases. However, it is not time to throw out everything humanity knows from previous designs and methodologies. One simple tweak is to accept the assistance CAD tools can offer.

Previous iterations of CAD tools have not really understood the holistic needs of designers well. If the tool is difficult to use, slow, inaccurate, and gives results that are hard to interpret, one can be assured that its adoption will be nil. However, some undesirable characteristics on their own are not necessarily deal breakers. The needs of a designer vary at different stages of the design process, the variation allows for trade-offs in the CAD tools to help maximize their effectiveness.

In the early stage of the design process, the designer might have an idea of a general area to search, say that of an electric motor or maybe even more specifically of an induction motor. The designer might know some rough parameters that are desirable, such as maximum dimensions or horsepower output. At this stage, it is desirable to quickly narrow the search space. Thus speed is the dominating factor over accuracy and results should be given in easy to understand global device parameters. Quick and easy to digest results allow for fast design iterations.

Somewhere in the design process, when the designer is satisfied that the search space is sufficiently narrowed, the speed versus accuracy trade-off shifts and begins to favor higher accuracy and detail. At this stage the designer wishes to spend more energy on focusing the search to precisely identify one or many possible solutions in the narrowed search space. It is assumed the first stage has yielded an area where a solution exists, thus feasibility is satisfied and expending more time and energy searching the area is acceptable. As the search progresses, the CAD tool now needs to give more and more detailed results. These results may come slower and be more complex, but allow for methodical refinement towards a viable solution.

As the bar of solution accuracy is raised progressively higher, a change in modeling technique may even be necessary. By the end of the process the designer wants assurance that the chosen design will function in reality as it does in the model. In cases such as a complicated induction motor design, this means incorporating precise material properties, very fine geometric discretizations, and understanding not only the magnetic field distributions in the motor, but also coupled phenomena such as thermal properties, stress distributions, etc.

A designer who can efficiently utilize all this information and assist the computer in knowing when to switch between design stages will undoubtedly be empowered by adopting CAD tools. It remains to be seen if a non-learned designer can manage this, but if history is indicative of how far humanity has progressed technologically, experience counts for something.

CHAPTER 2
History of the induction motor and its design

More than a decade ago, Boldea and Nasar stated that there are "more than 3 kW of electric motors per person" [6, pp. 1] in developed countries, predominately from induction motors. Since then that number has undoubtedly grown, as these extremely useful devices continue to pervade our everyday lives. With a multi-decade resurgence of research in the field, the century-old induction motor is undoubtedly slated to remain a fixture of modern life.

Independently invented by Galileo Ferrais and Nikola Tesla in the mid 1880s, induction motors provided an elegant way to convert alternating current to mechanical energy utilizing abundant materials and mechanically simplistic means. The unique innovation demonstrated by Ferrais and Tesla was the construction of a rotating magnetic field. Whereas previous solutions utilized mechanical means, commutators, to reverse current direction in rotor windings and progressively shift the device's magnetic poles, the induction motor instead achieved an equivalent phenomena innately using only careful winding placement and multiple phase AC.

The developments leading up to the discovery were observed experimentally by the scientific community as two phenomena: the so-called "Arago rotations" [7, pp. 285] and its inverse, the effect of induced current on a magnetic field. These rotations were observed by Francois Arago in 1824 when he noted that a magnetic needle suspended above a copper plate would begin to spin when the copper disc was spun. However, the scientific explanation given at the time was incorrect; in 1831 Michael Faraday experimentally disproved the theories of Charles Babbage and John Herschel and suggested that the revolving copper disk cut the lines of magnetic flux created by the permanent magnetic field in the needle, which in turn induced momentary currents, “eddy currents”, in the copper plate on either side of the needle. These momentary currents then created their own magnetic field which interacted with field of the needle and produced a force on the needle, causing it to spin with the disk [7, pp. 285-286].

While these discoveries demonstrated the principle of energy conversion by induced currents, it did not show how to use an external electrical source to provide the energy to power the conversion to mechanical energy. Practical applications of Faraday's explanation languished until nearly 50 years later when Walter Baily and Marcel Deprez independently discovered a means of producing a rotating magnetic field from an electrical source. Walter Baily's alternative “Mode of Producing Arago's Rotation” [8] in 1879 demonstrated a device with four electromagnets that were switched on and off in pairs by turning a commutator-like wheel to produce a rotating magnetic field. Baily notes in his 1897 publication that this is a simplification of the situation where one uses infinite electromagnets to produce a uniform rotating magnetic field, which is more or less analogous to the previous work done by Babbage and Herschel in 1825 who physically rotated a horseshoe [7, pp. 285-286].

The final attribution came from Marcel Deprez who took Baily's work just one step further and described how to electrically create a rotating magnetic field. Deprez explains in his 1883 paper [9] that the “l'action magnétique dirigée suivant la ligne des pôles,” magnetic action directed along pole lines, can be broken into components upon which coils could be placed. These coils could then be excited with two different currents of varying intensity to create, “une résultante dont la position dépendra du rapport des courants,” a resultant field direction that is dependent on the ratio of the currents.

Interestingly, Silvanus Thompson, an expert engineer of the time and author of many books [10, pp. 62], [11, pp. 703] that provide historical and technical context, attributes this “theorem” to Deprez, but departs from Deprez's descriptions for a much more mathematically rigorous explanation to which he references Ferrais. From a reading of Deprez's original publication it is easy to see how it went undiscovered with the conclusion essentially independently redrawn by Ferrais and Tesla for their own works, as Deprez's work was not widely circulated or known until the early 1890s [7, pp. 288]. In Deprez's paper there is discussion of a needle tracing out an arc between two poles which are separated in space by 90º, but nothing as explicit as given by Thompson or that would meet this author's definition of “proved mathematically” as described by Kline. It makes more sense for the needle displacement to be restricted and thus the discovery used to make an electric compass or measurement device rather than an electric motor.

Perhaps this historical footnote was added post hoc since Thompson's forth edition book "Dynamo-electric machinery" published in 1893 mentions Deprez's notion "that a rotating magnetic field might be produced by the combination at right angles of two alternating currents" [11, pp. 703] occurring in 1885 with no reference to Deprez's 1883 paper mentioned in later editions [10, pp. 63]. Perhaps some insight to this might be gleaned from a rather boorishly and completely unrelated anecdote left by Thompson – "It has been noisily claimed, but without the shadow of reason, for Marcel Deprez, who did not, however, discover it until..." [11, pp. 19]

Some modern historical analyses [13] of the rotating magnetic field issue credit Tesla for the discovery in 1882. Furthermore, the Muzej Nikole Tesle in Belgrade claims to have early drawings done by Tesla of two-phase and three-phase alternating current motors dated March 10, 1884 [14].

By the mid 1880's the battle between alternating current, AC, and direct current, DC, was ramping up. One of the things AC systems sorely lacked was a practical AC motor. While all motors are technically AC motors, those that existed at the time were not self-starting and had to be spun up before being energized. The commercial opportunity was glaringly obvious as evidenced by the ensuing patent battles following Tesla's patent [15], [16] filed on November 20, 1887.

Tesla filed a flurry of patents between October 1887 and their lumped assignment on May

1st, 1888. The patents very explicitly and with unmatched completeness covered creation of a rotating magnetic field by electrical means, motor types and topologies arising from this discovery, as well as other subsequent advancements such as those related to electrical distribution. Filings later in the aforementioned period show a true induction motor with short-circuited rotor windings, a commutator-less device; a feature Tesla claimed [17] he sought since seeing a the brutal sparking of commutator brushes on a Gramme generator being operated as a DC motor during a lecture demonstration in 1877.

Ferraris, on the other hand, published [18] the bulk of his discoveries in March of 1888 with an English translation [19] appearing in December of 1895. The original 17 page paper was broken into 6 parts: part 1 wasted no time in showing visually, verbally, and mathematically how a rotating field could be created by two alternating currents described by a sine function; part 2 described a device used for experiments in the autumn of 1885 built of a copper cylinder suspended inside two coils; part 3, mounted the rotor onto a bearing mounted shaft, enlarged the dimensions and made a practical AC motor; part 4 presented a mathematical model and suggested some novel measurement parameters to describe induction motor performance; part 5 concluded based upon the incorrect mathematical model presented in part 4 that the induction motor was not "of any commercial importance as a motor"; and finally part 6 presented an anecdotal experiment with a beaker of mercury as a rotor. Ferraris' thoughts on the subject were fatally flawed in predicting the induction motor to be a low-efficiency device, deterring him from further research on such devices [19, pp. 283], [7, pp. 289].

Tesla and others, however, continued work on commercialization of the induction motor; Tesla, after the award and subsequent sale of his patents, joined Westinghouse in 1888 and worked until 1889 with little success. After Tesla's departure from Westinghouse, Tesla's assistant, Charles F. Scott, redesigned the motors with a moderate degree of success, though commercially the product was a failure. The sorry commercial state of the induction motor languished until 1891 when Maschinenfabrik Oerlikon of Zurich and AEG of Germany demonstrated 20 and 100 horsepower induction motors, a far cry from Tesla's fractional horsepower fan motor and Scott's 3 and 10 horsepower motors. The engineers responsible for the 20 and 100 horsepower machines were Charles E. L. Brown and Michael von Dolivo-Dobrowolsky, respectively [7, pp. 292].

Brown and Dobrowolsky's success was a result of experimentation dating back to the mid-1888s after Dobrowolsky learned of Tesla's work [7, pp. 293]. During these experiments Dobrowolsky invented [20] a special “squirrel-cage” rotor made up of copper bars running through an iron rotor stack. The bars were short-circuited together by a ring at each end of the rotor [11, pp. 707], akin to Tesla's aforementioned short-circuited rotor coils. Other improvements came from the use of three phases instead of two, distributed windings in stator slots as opposed to salient poles, and the translational use from DC motors of rheostats to increase rotor resistance and decrease rotor inrush current during starting [21]. Kline attributes [7, pp. 294] the improvements to an experimental comparison Dobrowolsky did when sizing up a smaller 1/10 hp motor to 5 hp. It is also likely that his academic and industrial knowledge led him to an understanding of “magnetic circuit” theory, a design method gaining use during the time, which would emphasize the need to minimize leakage fluxes.

Brown's smaller motors became popular in subsequent part of the 1890s for their “inexpensive, rugged, and reliable” [7, pp. 294] nature since they didn't utilize any failure-prone pieces such as, slip rings or starting rheostats. Larger motors used Dobrowolsky's rheostat method to increase starting torque, but were also more expensive for this reason. S. P. Thompson includes a chapter titled “Some examples of modern polyphase motors” in his 1895 book [10, pp. 210-216], the pages are dominated by Brown's commercial offerings and only a paragraph dedicated to Westinghouse's Tesla motor. Whether this is due to Thompson's affiliation with the European locale or because Westinghouse's motor was less popular is unknown.

An American engineer who joined Westinghouse after Tesla's departure, B.G. Lamme, wrote a history [22] of the induction motor in 1921, which “covers principally those developments with which the writer [Lamme] has been in more or less personal contact” [22, pp. 203]. Lamme tells the mostly American side of developments from 1891 and onward. The paper sheds light on the timing and reasons for many developments with excellent historical context, though in the context of design processes the semi-autobiographical narrative provided by Lamme is perhaps the most valuable.

It is very evident by Lamme's writing organization that half a dozen companies across the world were all working on developing the induction motor, creating their own design methodologies, unique motor features and characteristics, and sharing as little as possible with each other. The latter taking the form of the discouraging statement [22, pp. 206],

> *It is one of the greatest misfortunes of the engineering profession that so few of the great pioneers and the development engineers have recorded the steps which have led to success or failure.*

The competitive nature of the time is best illustrated by Lamme's attendance at the 1893 World's Fair in Chicago, where Westinghouse's display was evidently "right across an aisle from" AEG [22, pp. 206]. Lamme of course noted a few of the features and inquired as to some "regulating characteristics" to which "the German engineer looked at him and replied – 'Ah, you are from the Westinghouse company', and he volunteered nothing further."

In comparing the 1890 and 1891 developments of Brown and Dobrowolsky to that of their overseas equivalents, it is evident that the Americans were behind due to Westinghouse's financial troubles and some legacy design choices, namely supply frequency and salient stator poles. The same advancements Dobrowolsky patented in late-1889 with his caged rotor were tried over 2 years later at Westinghouse in 1892. It is therefore historically interesting that P. L. Alger in his short 1976 article titled "The History of the Induction Motors in America" would attribute this discovery to Lamme, even going as far to note that Westinghouse and General Electric "signed a crosslicensing agreement in 1896" [23] to avoid litigation over the use of such caged rotor types.

The technological gap was short-lived as the 1893 World's Fair showed that the "Europeans and Americans were independently developing polyphase apparatus along very similar lines" [22, pp. 206]. The same year, "the induction motor business in this country [America] really got into motion" [22, pp. 207]. Only two years thereafter, in 1895, Lamme noted that "the polyphase motor had become pretty firmly established as a commercial device" [22, pp. 209].

The motor's rapid development over the 1893 to 1895 span was less and less subject to the woes of the "cut and try" method from the 1880's. Lamme goes to great length to illustrate the point that "many of the well known actions of the induction motor were fairly well comprehended as early as 1894 and '95" [22, pp. 212]. These analytical developments stemmed from the application of Maxwell's equations to the induction motor. The analyses done by Louis Duncan, Maurice Hutin, and Maurice Leblanc went beyond Ferraris and derived equations to much more accurately predict the performance curves of the induction motor [7, pp. 301]. However, further levels of abstraction were necessary to bring forth a suitable design method.

The evolution leading up to these analyses was a long time coming. In the mid-1880s the sentiment of the engineering community was well summarized by the preface dated June

1884 of Thompson's book on electric machines [12, pp. xii]:

> *Of the laws of induction of magnetism in circuits consisting partly of iron, partly of strata of air or of copper wire, we know, in spite of the researches of Rowland, Stoletow, Strouhal, Ewing, and Hughes, very little indeed. Our coefficients of magnetic permeability and magnetic susceptibility, though convenient as symbols, are little more than convenient methods of expressing our ignorance. We want some new philosopher to do for the magnetic circuit what Dr. Ohm did for the voltaic circuit fifty years ago. Until we know the true law of the electro-magnet, there can be no true or complete theory of the dynamo.*

The idea of a magnetic circuit arose repeatedly as researchers attempted to simplify the magnetostatic models rooted in the mathematically-heavy first principles of Ampere's and Faraday's laws. Translating the mathematical meaning into tangible devices proved to be nontrivial for designers. Many hoped, as Thompson said, for someone to step forth and propose a set of simplified equations to distill the knowledge from a distributed field model into a lumped parameter model, akin to the electric circuit.

In 1855 a theoretically complete magnetic circuit was put forth by Maxwell that gave mathematical representation to Faraday's intuitions and analogies. Maxwell derived his magnetic circuit by the representation of magnetic flux as a slow incompressible fluid flowing through a linearly resistive medium. He further defined the interrelation of electrical current and magnetomotive force, describing all the requirements of its basic modern equivalent [24, pp. 160]. However, as Jordon notes, the work remained unnoticed as the applications to which the magnetic circuit would be applied had yet to be created.

By 1886 much debate had occurred as designers sought to create better devices, but the study of such devices remained largely akin to that of a black box; as discussed above the very literal “cut and try” method was standard procedure; the only quantified and measured parameters were the input and output. In the spring of 1886, John and Edward Hopkinson published their “rendering of the magnetic equivalence circuit, which was theoretically complete, structurally simple, articulated a wealth of detail, and had proved itself in the practical design of dynamos” [24, pp. 138]. The latter being the most important as the Hopkinsons likely applied their analytical methods to designs for Edward Hopkinson's employer, Mather and Platt. Jordan notes, as is highlighted above in Lamme's paper on the closed-door nature of commercial competition, that “Hopkinson kept much to himself about these design methods” [24, pp. 140].

During the same time as the Hopkinsons, Gisbert Kapp presented his solution to the magnetic circuit in stages starting in 1885. As an “accomplished writer and speaker, and an important expositor and synthesizer of electrical engineering knowledge” [24, pp. 142], Kapp's solution [25] sparked great debate for a number of issues, but its acceptance within a few short years was quite swift. Jordan presents a quote, which provides ample insight to its acceptance even among such animosity from others. One professor, William E. Ayrton, remarked that the paper was “of great interest, because it has placed the results of experiments in a form both practical and suitable for engineers to use... [It was] rather stranger that [designers] had not at their fingers' end the information that would enable them to foretell the output from a dynamo" [24, pp. 146].

While all of these developments happened prior to Tesla's first tangible induction motor, they provided the basis for further analytical developments in the 1890's. The significance cannot be understated as Jordan concludes by quoting John Perry, an assistant to Lord Kelvin and later professor [26, pp. 581]:

> *I think, however, that it is my duty, even now, to point out that this paper of Mr. Kapp's is really, in quite an exceptional matter, a very useful one, for by the method described in it we can calculate the characteristics of a dynamo in a most straightforward way from the beginning to the end without difficulty, so that even the youngest member of the Society, in dealing with dynamos, can make the calculation. Mr. Kapp has with great clearness put forward his whole method, and the principles underlying it. In a manufacturer, such a course of action is exceptional, and he has well earned our gratitude. Others may have anticipated him, using a method somewhat similar to his, but Mr. Kapp was* ***the first to make this valuable practical method of calculation public property*** *[emphasis].*

Looking again at analyses of the induction motor in the early-1890's; such as those put forth by the aforementioned Louis Duncan, Maurice Hutin, and Mauirce Leblanc; time has shown that relationships found between machine parameters is correct, however, the method fails to accurately predict machine performance. Kline notes that this is due to Maxwell's treatment of induction coefficients as constant, the derived work thereby making the same assumption. With iron being a main component of induction machines, this assumption ignored effects of hysteresis, eddy currents, and variable permeability; having an irrevocable affect on its accuracy [7, pp. 307].

In 1894 by combining the theory of Maxwell; complex number analysis of AC-systems; the abstractions of Hopkinson and Kapp; and improving upon the work of Duncan, Hutin, and Leblanc; Kapp and Charles P. Stienmetz put forth an induction motor model that aptly “eliminated these coefficients by modifying traditional magnetic circuit theory with two new parameters borrowed from their transformer theories: 'leakage inductance' and 'primary admittance'” [7, pp. 306]. The hybridization of methods and the way in which these new non-empirical parameters were defined gave rise to a much more accurate representation of the losses caused by leakages, hysteresis, and eddy currents.

One example of the other methods competing with Kapp and Steinmetz's theory was the “circle diagram” created independently by Alexander Hayland and Bernard Behrend [27], [28]. The graphical method utilized two empirical coefficients and Behrend's leakage coefficient in order to graphically complete the required vector algebra and thereby calculate machine performance parameters. The method remained into the 1950s, when one imagines the advent of computers heavily favored the methods of Steinmetz [7, pp. 309].

Improvements to Kapp and Steinmetz's work came with the publication [72] by Steinmetz of his transformer equivalent circuit in 1897 [23, pp. 1381]. Anecdotally, Klein notes [7, pp. 308] that Steinmetz did not publicly apply his equivalent circuit to the induction motor until 1917, but others undoubtedly saw the connection to the induction motor well before then. The development of the equivalent circuit allowed any induction motor design to be connected and simultaneously analyzed in conjunction with other devices on the same network using circuit theory.

The final semi-mathematical design method used by designers from the beginning of induction motor design are their uniquely developed empirical equations. These equations related parameters to dimensions and various operational characteristics of related motors, as well as empirical corrections to the more analytical and universal induction motor theory. Few papers were published with these types of equations, design rules, or data; those that were, were authored mainly by academics; as the knowledge was and still is well protected in the vein of competition.

With engineers working for dozens of companies large and small spread across the world, many of the discoveries and much of the knowledge was very likely discovered repeatedly in silence. For example Lamme describes that in 1895 and 1896 he moved from graphical solution methods to “mathematical equations, derived directly from the geometry of the vector diagrams” [22, pp. 214]. By “analyzing magnetic conditions, with a view to predetermining all the 'leakages' or 'stray fields', etc. and checking with existing machines” he was able to “reproduce, by calculation, the reactance conditions of practically all the existing machines” [22, pp. 212-213]. Nowhere in that specific section of the article does Lamme mention Kapp or Steinmetz. Instead three pages later he, with little deference, mentions the work of Steinmetz in the context of the era being the

“'Golden Age' of induction motor development” [22, pp. 216]:

> *During this time [1894 to 1900] the theory of the induction motor was worked out and applied in practical forms of calculation, and the methods of calculation, developed in that time, hold with slight modification until today [1921]. The method of analysis and calculation derived by the writer in connection with the development of the cage tyyp [sic] motor, as already described was used throughout the following years by the Westinghouse engineers and is the basis of their present methods. In the General Electric Company the methods devised by Dr. C. P. Steinmetz, during this period, are also used very generally throughout that company. These methods are naturally very closely related to each other, although expressed in somewhat different form.*

It is rather ominous that Lamme commented on the achievements of the afore-described era as being so successful that there had been no “radical departures” in the type of induction motors built 25 years later in 1921 [22, pp. 216].

> *Indeed this period might be called the “Age of Induction Motor Analysis,” as well as development, for practically all the modern analysis is based upon fundamentals developed during this time. All the analytical work was not published, but the methods of those times were carried into practical fields, with marvelous results, and it may be said that methods of today are largely refinements of those twenty years ago. These refinements have led to refinements in the machines, but not to any new principles which have allowed any radical departures in types.*

Considering Steinmetz's equivalent circuit remains a facet, if not the facet, of nearly every induction motor textbook one can read in 2013, one can only assume that the methods of Lamme, Steinmetz, and the many silent others remain in use in one way or another today.

For further evidence that Lamme's words remain true well after his article and death, see P. L. Alger and R. E. Arnold's article [23] from 1971. The article curtly details the history and developments of the induction motor, from Tesla to Westinghouse and General Electric. The article features an ingratiating paragraph on Steinmetz and his analysis method, the only analysis method mentioned, with the rest of the article dedicated to advancements on new starting methods, cast rotors, magnetic steel, conductor insulations, overload devices and the effect on increased output ratings. In no way is a "radical departure in types" seen, as Lamme indicated, rather a steady "refinement in the machines" as materials improved.

If Lamme could publish his article in 2013, he would undoubtedly begin it in much the same way, bemoaning the silence of his fellow engineers in telling of their successes and failures. Rather oddly he would probably conclude in much the same way as to say that the methods of the "practical fields... of today are largely refinements of those of ~~twenty years ago~~ [strikethrough]" [22, pp. 216] over a century ago.

CHAPTER 3
First principles and reduced-order models

3.1 Electric machine modeling methods

The effectiveness of analytical methods in industry notwithstanding, the research world has focused on new developments with the advent of modern computing. Currently, in the world of electric machine design, stand two seemingly distinct analysis methods: the mathematically complex finite element method, FEM, and the comparatively reduced-order, pragmatic magnetic equivalent circuit, MEC. Through decades of research each method has reached a level of fluency, FEM more than MEC, such that carefully obtained FEM and MEC results are able to describe certain phenomena and match global machine parameters measured in experiments.

The FEM provides a general mathematical framework with which to apply first principles, i.e. equations governing electromagnetics, to a discrete geometry without any a priori knowledge. The method has reached a certain maturity in engineering as seen in the volumes of work that have been done to research, understand, and document how to use finite elements to solve many types of problems. In the field of electric machines starting with Silvester [35, pp. 223-225] and Chari's publication in 1970, work on applying the FEM to these devices has been substantial with entire textbooks dedicated to the subject [37] and commercial products [29]-[33] that cater to solving the field problems presented by such machines.

By solving Maxwell's equations directly with the FEM, the designer gains automatic inclusion of many effects that are ignored and empirically accounted for in analytical methods, for example leakage inductance and harmonic effects [38, pp. 21]. The geometric basis that provides this advantage by working with the lowest level of abstraction, the fields, is also the biggest disadvantage as the complexity of the calculations can quickly become time prohibitive to solve. In addition once the field solution is obtained, more calculations are necessary to find the motor parameters used to compare against other designs, simulation methods, and experimental results.

For these reasons and the fact that a designer has to explicitly specify the geometry, the FEM is rarely used as the primary design tool, instead it is more commonly “used to calculate the detailed performance of a previously engineered machine” [38, pp. 21]. However, in cases of novel designs where no accurate analytical technique exists, working from first principles with the FEM is the only option. The granularity in the types of analysis, innate inclusion of as many phenomena as needed, and the ability to provide a solution as accurate as computation time allows, uniquely sets the FEM apart from analytical methods. It is noted that the FEM is not the only method used in previous works, the finite difference and boundary element methods do exist and are widely used; however, the finite difference method can be considered a 0-order finite element method and the boundary element method is generally less favored than the FEM when nonlinear and transient analysis are needed.

On the other hand, the MEC, a lumped parameter network, works a posteriori by utilizing only Faraday's and Ampere's laws, as well as physical and geometric assumptions derived from the designer's tacit knowledge of the flux paths being represented. It is the a posteriori knowledge in these assumptions that cause the MEC to retain accuracy, but reduce computational complexity.

While there has not been nearly as many researchers working on the MEC, its first developments can be seen as an amalgamation of the basic magnetic circuit principles of the 1880's and the work of Laithwaite [39] and Carpenter [40]. Amrhein attributes [38, pp. 22] the "first useful MEC application" to "Faucher in 1982," though the bulk of knowledge about the MEC remained scattered until Ostović published his book [47] based upon his journal publications[42]-[46] and PhD thesis [41]. Since the book's publication in 1989, the MEC has begun to appear more frequently in literature as many sought to improve upon Ostović's work.

Many papers exist applying the MEC to the induction motor analysis problem. Amrhein in his PhD thesis references the work of Sewell et al. [48], Perho [49], and Sudhoff et al. [50]. In more recent personal communications with Amrhein, the work of Bash et al. [51] and Derbas et al. [52] was recommended. While the latter two papers are not directly applied to the induction motor they represent some of the current ideas on the MEC. Yilmaz, who shares the same supervisor as Amrhein, has published a metapaper [53] comparing papers which performed MEC analysis against FEM or experimental results.

While most show agreement with the FEM or experimental results, the multitude of assumptions and MEC implementations for real devices, in this author's opinion, lack a certain transparency seen in the more rigorously defined algorithms of the FEM.

The inherent lack of rigor in the MEC makes following and replicating the results of literature difficult for a number of reasons. Firstly, the MEC's geometric basis is much more loosely defined because the shape of the device and its flux paths are fit to the MEC element, whereas in the FEM, one could argue that the elements are fit to the shape. Secondly, the MEC mesh generation is very dependent on the individual designer's preferences with an arbitrary mesh generator being nonexistent or possibly impossible. These negatives are also the MEC's greatest features as it allows a designer to provide knowledge that directly results in lower computation complexity with only minimal loss of accuracy, given “correct” knowledge.

Another way designers can use their knowledge is by selecting which phenomena they wish to incorporate into their model and how to do so most efficiently. Literature provides a few possible ways a designer can attempt to get the best out of the FEM, MEC, and electrical equivalent circuit, EES, by modeling different components with different methods, so called hybridization [54] or coupling [55], [56]. For example Gyselinck et al. [54] compare the effect upon the operation of an induction motor when its feed, a three-phase transformer, is modeled by FEM, MEC and EES. The paper notes that when using only EES, the magnetic interactions between the three-phases in the transformer are not taken into account and that performance change is not translated into the induction motor results. Interestingly, the paper finds a certain congruence when using FEM and MEC, as both methods take the interaction phenomena into account.

Other papers by Dular [57] follow in a similar vein, but apply perturbation methods to FEM formulation. In this case, Dular solves three problems in order to get one final field solution, one of which corresponds to the formulation for ideal flux tubes, the same idea used in derivation of the MEC. Further indication that the FEM's generality could somehow be constrained and reduced in complexity to act as the MEC.

Finding a certain similarity in the results from FEM and MEC is a common theme in many papers [53]. Even from the rebirth of these lumped parameter methods, Ostovic in his 1988 publication [44] on an MEC for the induction motor concluded, “the magnetic equivalent-circuit method, being essentially a kind of finite-element analysis...” With that sentiment a somewhat trite exploration into what conditions could be applied to the FEM to reduce it to MEC was completed and is presented below.

3.2 Combining the magnetic equivalent circuit and finite element method

The reader is referred to any primer on the finite-element method for the derivation and basic principles, which are not repeated here. A popular reference for FEM in electromagnetics by Jin [63], from which the FEM equations used below are taken. For the MEC related primers see the PhD thesis of Amrhein [38, pp. 30-33] or Ostović's book

[47, pp. 6]. Note the method and notation of Amrhein is used in derivation of the MEC below.

3.2.1 Magnetic equivalent circuit

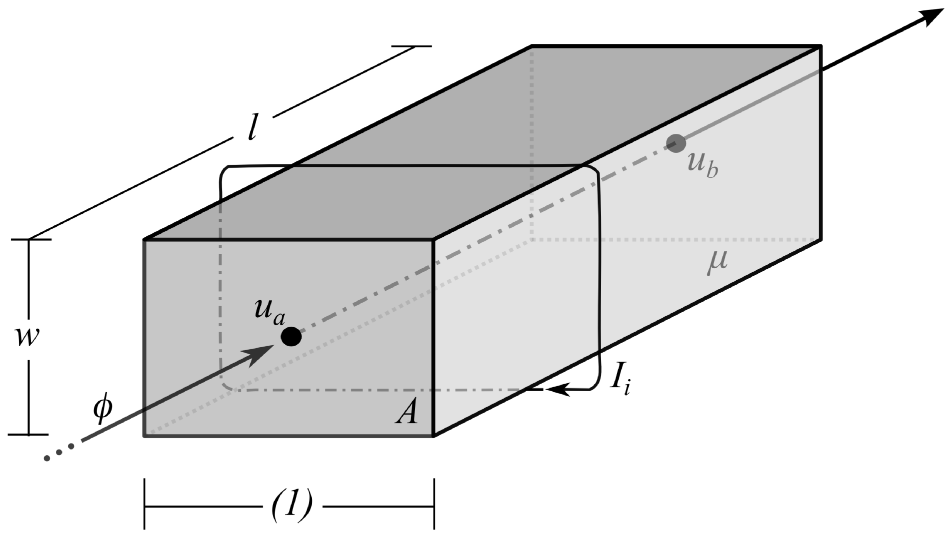

Fig. 1: The basic MEC element, adapted from page 32 of [38]

As previously mentioned, the MEC can be derived from Ampere's and Faraday's law, given a few assumptions. The first of which is that wave phenomena can be neglected as the frequency of excitation compared to the dimension is small. The derivation begins by first examining Ampere's Law

$$\oint_C H \cdot dl = \iint_S J_i \cdot dA \tag{1}$$

where "H is the magnetic field intensity and J_i is the imposed source current density" [38, pp. 30]. That is the current density created solely by electric current encircling the element, neglecting eddy currents in this basic version of the MEC. While this may be discerning considering the application of the MEC to the induction motor, the pure flux method presented can later, through flux linkages, be connected to the electrical system of a machine, for example to model the currents in the rotor bars and their effect on the rotor teeth and core fluxes.

Define a magnetic scalar potential, *u,* as

$$\boldsymbol{H} = \nabla u \tag{2}$$

Combining (1) and (2) under the assumption that the only imposed current density present is from a conductor with current I_i surrounding the circumference of the element yields,

$$\oint_C \nabla u \cdot dl = \iint_S J_i \cdot dA = I_i \tag{3}$$

It is advantageous to begin introducing lumped parameters to simplify and abstract away from having to work with the field parameters directly. Therefore the magnetic motive force, MMF, is defined from location *a* to *b as* F_{ab}, as shown in Fig. 1.

$$F_{ab} = \int_a^b \nabla u \cdot dl - I_i = u_b - u_a - I_i \tag{4}$$

Since the path C in (1) is defined as a contour, summing all the MMF across the path yields

$$\sum_{C} F_C = 0 \tag{5}$$

As with electric circuits, (5) is a form of Kirchhoff's voltage law, KVL. Such conditions are beneficial to satisfy as knowledge of solution methods used for electric circuits can be easily translated. In order to find Kirchhoff's current law, KCL, for the MEC consider magnetic flux density, B, and the integral form of Gauss's Law for magnetism,

$$\oiint_{S} \boldsymbol{B} \cdot dA = 0 \tag{6}$$

Naturally, magnetic flux density, B, is related to magnetic field intensity, H, by the permeability of the material in which the field exists.

$$\boldsymbol{B} = \mu \, \boldsymbol{H} \tag{7}$$

Substituting (2) into (7) and the result into (6), KCL is realized.

$$\oiint_{S} \mu(\nabla u) \cdot dA = 0 \tag{8}$$

Again it is helpful to abstract this into a lumped parameter, the integral of the magnetic flux density across the surface, *S*, is termed the magnetic flux through a surface or ϕ_S.

$$\phi_S = \iint_S \mu(\nabla u) \cdot dA = 0 \tag{9}$$

Such that (8) reduces to

$$\sum_S \phi_S = 0 \tag{10}$$

Amrhein notes [38, pp. 31] that the derivation of KCL is needed to model materials with flux sources, such as permanent magnets.

At this point in the derivation, few assumptions have been put upon the equations, to abstract it further away from the field representation and closer to that of a lumped parameter network, it is helpful to introduce the intermediate idea of the tubes and slices method [61], [60]. While a slight digression, Hammond and Sykulski's method [59, pp. 4] helps illustrate the mechanics of the MEC through a much simpler problem, calculating the inductance of a piece of material.

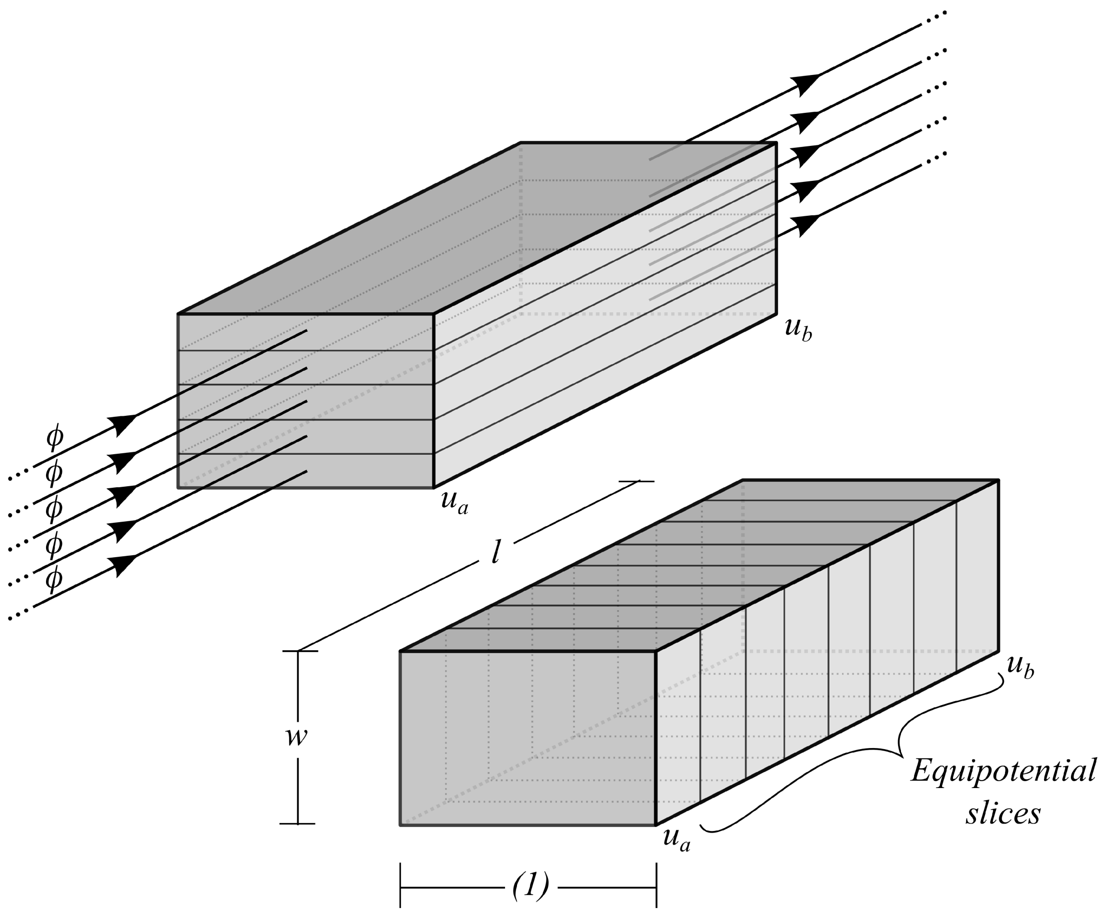

Fig. 2: Tubes of equal flux [top], slices of equipotential [bottom]

3.2.2 Tubes and slices

Consider a cuboid of iron with an MMF imposed across the vertically facing faces, ie from *a* to *b*. The flux runs perpendicular to the MMF faces through the iron. As the flux pushes through the iron, it experiences the MMF difference seen mathematically in (4). As it progresses the current MMF potential becomes closer and closer to the potential at *b*, these intermediate walls of potential are referred to as "slices" [59, pp. 4]. The walls conform to the equipotentials surfaces of the field, meaning the MMF at every point on the slice has the same potential as every other point on the same slice wall. Conversely, consider the path which the flux follows from *a* to *b*. Instead of an infinitesimally small line, consider if the iron itself was subdivided into infinitesimally thin sheets through which flux flows. These “tubes” [59, pp. 4] uniformly distribute and contain the flux such that it never interacts with any other flux sheet, but are devised in such a way that they do not change any of the flow characteristics. By definition the tubes and slices are always perpendicular to each other at every point, even through the geometry need not necessarily be rectangular.

In order to make useful calculations, one needs a graphical field solution showing the tubes and slices. By applying the rule that the tubes and slices need always be perpendicular and propagating the tubes and slices from the boundaries, a graphical field solution can be constructed through trial and error.
Hammond and Sykulski [59, pp. 55] do not apply their method to electrical machines, but instead to calculating the permeance.

A measure of flux per current-turn, permeance, represented by *P*, is commonly referred to as being analogous to conductance in electric circuits. It is defined as the ratio of flux to MMF,

$$\phi = P \cdot F \tag{11}$$

Consider now the small rectangular-like section with depth enclosed by the walls of two tubes and the walls of two slices. It is known that at wall x_1 there is a MMF, F_1, and at wall x_2 there is a MMF, F_2. The walls of the tubes have sides at y_1 and y_2 and depth from z_1 to z_2. Assume the permeability to be constant in the section and the magnetic scalar potential, u, to be only a function of x. Additionally, the piece has overall length l and cross-sectional area A. Equation (3), KVL, reduces to,

$$\oint_l \mu(\nabla u)\cdot dl = \nabla u\cdot l + u_2 - u_1 = I_i \tag{12}$$

Equation (8), KCL, reduces to,

$$\oiint_A \mu(\nabla u)\cdot dA = \mu\cdot A\cdot\nabla u = \phi \tag{13}$$

Rearranging (11),

$$\frac{I_i + u_1 - u_2}{l} = \nabla u \tag{14}$$

Substituting (14) into (13),

$$\phi = \frac{\mu\cdot A}{l}\left(u_1 - u_2 + I_i\right) \tag{15}$$

Noticing that the last part of (15) corresponds to the MMF, the remaining terms must be the permanence to fulfill (11).

$$P = \frac{\mu \cdot A}{l} \tag{16}$$

As mentioned, Hammond and Sykulski use the result to subdivide a geometry using the above rules and then measure each appropriately subdivided piece to calculate a permeance. By considering each piece of tube to be in series and then each slice in parallel, or vice versa, an approximated permeance is found. Any consideration of current is unnecessary, however it is noted that the inductance of a structure can be found using this method as they define inductance as merely flux over the MMF, the same as the permeance [59, pp. 55].

The accuracy of such methods is reasonably comparable to FEM results, as is demonstrated by Hammond and Sykulski throughout the book. Overall the assumptions made in the derivation, namely the constraints put upon the field hold well, however nowhere near as well as in electric circuits. The reason is the relative material properties at material interfaces. In an electric circuit, the difference in conductances between non-conducting air and conducting copper is very high, on the order of 10^6, where as in a magnetic circuit, the difference from vacuum to a material considered flux-carrying like iron is rarely greater than 10^4 [47, pp. 9]. The smaller difference means that flux is held onto less tightly by iron and is therefore free to take a possibly easier path even though the material can intrinsically carry less flux. The leakage is not taken into account directly as in the FEM, but can be introduced with MEC elements spanning areas of potential flux leakage.

While many parts of the magnetic circuit can be seen as analogous to the electric circuit, the comparison if taken literally can dangerously misrepresent the physics at play. In the electric circuit governed by conductance, the inverse of which is resistance, energy is literally lost as heat due to the material's resistance to electric current, thus reducing the potential. However in the magnetic case, the material property is permeability, which is a measure of how well a material supports a magnetic field. This can be viewed more tangibly for its role in defining how much energy can be stored as magnetic field in the material, since inductance and permeance are a function of permeability. A basic result from electric circuits is that an inductor, *L*, can store energy equal to,

$$E_L = \frac{L I^2}{2} \tag{17}$$

ignoring any magnetic saturation effects, the higher the permeability, the higher the inductance, the more energy that can be stored. Interestingly, the permeance only depends on geometric and material parameters, making it or its inverse, the reluctance, equally easy to calculate.

$$R = \frac{1}{P} \tag{18}$$

3.2.3 Finite element method

Now that the MEC element has been derived, an examination of the FEM is needed to see how to place the same conditions of Hammond and Sykulski's tubes and slices method upon the FEM elements. For the sake of simplicity two triangular elements with linear basis functions will be used, as that is all that needed to model the complexity of the MEC element. Jin's derivation for magnetostatics is unable to model flux sources in its current form [63, pp. 119], thus to include this phenomena the methods similar to Weiss et al. [62] have been introduced in the form of a one-dimensional element "cut". In the "cut" domain the equivalent current density created by current flowing around the element (Fig. 1), J_i, is zero and a "current sheet" that represents the "uniform magnetization of the permanent magnet" is substituted with an equivalent current density, J_M [62]. The permanent magnet material is not shown in Fig. 1, but is alluded to in the derivation KCL for the MEC, (10). A more detailed treatment of flux sources is given in [47] and [38].

The classical definition of the the magnetic vector potential for 2-D used below, A_z, is defined differently than the magnetic scalar potential used above, u, however their relationship is shown below with respect to MEC parameters. That is that a difference in u is MMF potential and a difference in A_z is magnetic flux. Jin's terminology is adopted here forth to distinguish between the MEC and FEM steps with a few substitutions to avoid confusion between the terminology used in Jin's general FEM derivation and the terminology for the magnetostatic case.

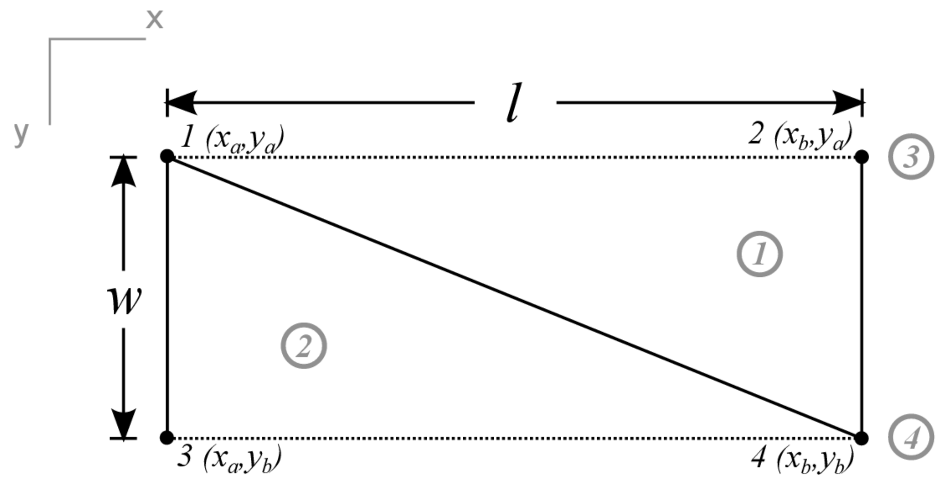

Fig. 3: 2D FEM discretization of basic MEC element. Dashed lines indicate 1-D "cuts."

$$\nabla\times\left(\frac{1}{\mu}\,\nabla\times A_z\,\hat{z}\right)=\left(J_i+J_M\right)\hat{z} \tag{19}$$

Where A_z is defined in relation to the magnetic flux density, B, as

$$\boldsymbol{B}=\nabla\times\left(A_z\,\hat{z}\right) \tag{20}$$

Given Fig. 3, the nodal coordinates and nodal element compositions can be written as

node	*x−coord*	*y−coord*
1	x_a	y_a
2	x_b	y_a
3	x_a	y_b
4	x_b	y_b

element	*nodes*
1	1, 2, 4
2	1, 3, 4
3	1, 2
4	3, 4

(21)

The FEM used below uses only triangular elements with linear basis functions because that is all that is needed to satisfy the degrees of freedom in the MEC system. Working the FEM through by hand, the linear shape functions are given by,

$$N_j^e(x,y) = \frac{1}{2\Delta^e}(a_j^e + b_j^e x + c_j^e y) \qquad j = 1,2,3 \tag{22}$$

Where the exponent, *e*, is the element number; the subscript denotes the *j*-th shape function; Δ^e is the area of the element defined in (25) below; and the coefficients *a*, *b*, and *c* for triangular elements 1 and 2 (Fig. 3) are given in below in (23) and (24), respectively [63, pp. 96].

$$\begin{array}{lll} a_1^1 = x_b y_b - y_a x_b & b_1^1 = y_a - y_b & c_1^1 = 0 \\ a_2^1 = x_b y_a - y_b x_a & b_2^1 = y_b - y_a & c_2^1 = x_a - x_b \\ a_3^1 = x_a y_a - y_a x_b & b_3^1 = 0 & c_3^1 = x_b - x_a \end{array} \tag{23}$$

$$\begin{array}{lll} a_1^2 = x_a y_b - y_b x_b & b_1^2 = 0 & c_1^2 = x_b - x_a \\ a_2^2 = x_b y_a - y_b x_a & b_2^2 = y_b - y_a & c_2^2 = x_a - x_b \\ a_3^2 = x_a y_b - y_a x_b & b_3^2 = y_a - y_b & c_3^2 = 0 \end{array} \tag{24}$$

The area of each element, Δ^e, where the *e* exponent designates the element number, is given by the equation,

$$\Delta^e = \frac{1}{2}(b_1^e c_2^e - b_2^e c_1^e) \tag{25}$$

The elemental stiffness matrix entries are given by the formula [63, pp. 98] with substitutions relating to the magnetostatic case [63 pp. 119] for the triangular elements

$$K^e_{jk} = \frac{1}{4\,\Delta^e \mu}\left(b^e_j b^e_k + c^e_j c^e_k\right) \tag{26}$$

And the triangular element contribution to the right hand side of the FEM system, designated by a non-italic b,

$$\mathrm{b}^e_j = \frac{\Delta^e}{3} J^e_i \tag{27}$$

Note that J_i in element 1 is pointing in the postive z-direction and in element 2 in the negative z-direction. It is important to remember that the derivation seeks to model the MEC using the FEM with the same degree of complexity; it does not seek to accurately model the real device directly, which results in some otherwise nonsensical application of parameters. The issues arise from the hand-waving treatment of sources in the MEC compared to the FEM. In order to model the sources in the FEM, the location of the elements containing the current density and their geometric information is essential and required information. Typically the flux carrying medium does not contain the current density and is simply excited by other elements or boundary conditions. On the other hand, the MEC disregards all the geometric information required to calculate the double integral in (1), instead quickly concluding that there is some surface associated with the MEC element that integrates to I_i, the current in the wire surrounding the element. By doing so it ignores the specifics of where exactly the current is located, the current density in the conductor, and associated phenomena.

Working from Ampere's law and applying the geometric information, the “cut” one-dimensional line elements contributions are found,

$$\frac{1}{\mu(y_a - y_b)} \begin{bmatrix} 1 & -1 \\ -1 & 1 \end{bmatrix} \begin{bmatrix} A_{Z1} \\ A_{Z2} \end{bmatrix} = \frac{l}{2} \begin{bmatrix} J_{M1} \\ J_{M1} \end{bmatrix} \tag{28}$$

$$\frac{1}{\mu(y_a - y_b)} \begin{bmatrix} 1 & -1 \\ -1 & 1 \end{bmatrix} \begin{bmatrix} A_{Z3} \\ A_{Z4} \end{bmatrix} = \frac{l}{2} \begin{bmatrix} J_{M2} \\ J_{M2} \end{bmatrix} \tag{29}$$

Since all the coordinates are now in terms of a difference, it is advantageous to define these differences in terms of length, *l*, and width, *w*,

$$\begin{aligned} l &= x_a - x_b \\ w &= y_a - y_b \end{aligned} \tag{30}$$

Calculating and assembling the global stiffness matrix and right hand side,

$$\frac{1}{2\mu w l} \begin{bmatrix} l^2+w^2+2l & -w^2-2l & -l^2 & 0 \\ -w^2-2l & l^2+w^2+2l & 0 & -l^2 \\ -l^2 & 0 & l^2+w^2+2l & -w^2-2l \\ 0 & -l^2 & -w^2-2l & l^2+w^2+2l \end{bmatrix} \begin{bmatrix} A_{Z1} \\ A_{Z2} \\ A_{Z3} \\ A_{Z4} \end{bmatrix} = \frac{lw}{6} \begin{bmatrix} 0 \\ J_i \\ -J_i \\ 0 \end{bmatrix} + \frac{l}{2} \begin{bmatrix} J_{M1} \\ J_{M1} \\ J_{M2} \\ J_{M2} \end{bmatrix} \tag{31}$$

Applying the knowledge that the potential at nodes 1 and 2 are equal and nodes 3 and 4 are equal, as shown by the equipotential edges drawn in Fig. 1, (31) reduces to,

$$\frac{1}{2\mu w l} \begin{bmatrix} l^2 & -l^2 \\ -l^2 & l^2 \end{bmatrix} \begin{bmatrix} 2\mathrm{A}_{Z1} \\ 2\mathrm{A}_{Z3} \end{bmatrix} = \frac{lw}{6} \begin{bmatrix} J_i \\ -J_i \end{bmatrix} + \frac{l}{2} \begin{bmatrix} 2J_{M1} \\ 2J_{M2} \end{bmatrix} \tag{32}$$

Writing out and simplifying,

$$\frac{l}{\mu w}(A_{Z1}-A_{Z3}) = J_i \frac{l w}{6}+(J_{M1}-J_{M2})\cdot(1)\cdot l \tag{33}$$

Recall a per unit depth has been assumed, a 1 has been added to the J_M term to note dimensional congruence between the terms on the right hand side of (33). Comparing with the MEC, (16) and (18), the length over the permeability and width is the reluctance. The difference of A_Z's multiplying the reluctance looks a lot like the flux, it is in fact by definition. To check, recall Amrhein's definition of the flux, (9), and apply the knowledge of tubes and slices where *B* is always perpendicular to the surface *dA* along the slice,

$$\phi = \iint \boldsymbol{B}\cdot dA = |\boldsymbol{B}|\, w \tag{34}$$

The definition for *B* when using the 2-D vector potential, A_z, simplifies to,

$$\boldsymbol{B} = \nabla\times(A_Z\hat{z}) = \frac{\partial A_z}{\partial y}\ \hat{i} + \frac{\partial A_z}{\partial x}\ \hat{j} \tag{35}$$

Because of the assumptions placed upon the potentials, the partial with respect to the x-direction is zero. Thus the definition for *B* as the curl of A_Z reduces to a one-directional field, here forth treated as a magnitude since direction is implicit in the MEC. Since A_Z is being modeled by linear basis functions in the FEM used above, the reconstructed solution for A_Z is a plane defined by the coordinates of the three nodes of the element and their respective solved A_Z values. In order to take the partial derivative the constants, *C*'s, for the following equation need to be found.

$$A_Z = C_1 x + C_2 y + C_3 \tag{36}$$

Solving for the equation of the plane, rearranging into form of the equation above, and taking the partial with respect to the y-direction of (36) yields,

$$\frac{\partial A_Z}{\partial y} = C_2 = \frac{A_{Z1} - A_{Z3}}{y_a - y_b} \tag{37}$$

Substituting into (35) and noting again that the partial with respect to the x-direction is zero,

$$|\boldsymbol{B}| = B = \frac{\partial A_Z}{\partial y} = \frac{A_{Z1} - A_{Z3}}{y_a - y_b} = \frac{A_{Z1} - A_{Z3}}{w} \tag{38}$$

Thus the flux can be found in terms of A_Z as,

$$\phi = |\boldsymbol{B}|\, w = B w = w \frac{(A_{Z1} - A_{Z3})}{w} = A_{Z1} - A_{Z3} \tag{39}$$

Which shows that the difference of the A_Z's is in fact the flux between those two points.

The remaining right hand side of (33) must be the MMF terms as seen in (15). Relating these terms between the two methods is a bit nontrivial as discussed above. Mathematically speaking, in the flux carrying medium with a current density of zero, (19) reduces to Laplace's equation, which is the governing equation for the field in the MEC element. In the FEM, under the assumptions that have been made above regarding the value of J_i in each element, the governing equation is Poisson's equation. Given the assumptions on the field, namely that the variation of A_z with respect to the y-direction is the only nonzero contribution, Poisson's equation (19) can be solved analytically for an element.

$$\frac{\partial^2 A_z}{\partial y^2} = \mu^{-1} J_i \tag{40}$$

Integrating to find A_z yields,

$$A_z = \mu^{-1} J_i y^2 + C_a y + C_b \tag{41}$$

Where C_a and C_b are constants of integration. The analytical analysis shows that direct solution of the physics give an equation that is of polynomial order 2. Whereas in the FEM above, linear basis functions are being utilized to approximate the analytical solution, forcing the FEM solution to be linear. Including the current density inside the FEM element creates this issue, however, looking at the FEM solution it is possible to manipulate the arbitrary J_i to force equivalent to the MEC. Manipulating J_i in this fashion is nonsensical in any real device, but removing the dependence of the FEM upon all the geometric information required to define a source is non-trivial.

Another possible way to apply J_i over the FEM elements would be to have a delta function with value of half $\pm I_i$ at nodes 2 and 3. Equation (27) would have to be evaluated from its definition since the value of J_i would not be constant over the element. Though this definition might break previous assumptions in the FEM derivation done by Jin. A second way would be to add a linear 1-D element along nodes 1 and 3, then J_i inside the actual triangular elements would be set to zero. Further research is needed to find which is "the best" or "least nonsensical" manipulation of J_i that yields equivalence.

Taking the first term of the right-hand side of (33) and setting it equal to I_i of the MEC. The nonsensical definition for J_i which achieves equivalence can be solved for as,

$$J_i = \frac{6 I_i}{l w} \tag{42}$$

The definition for the current sheet J_{M1} and J_{M2} given by the 1-D "cuts" is slightly more concrete. Applying the definition given (1) and (4), which relates a current density of a MMF,

$$\int_0^1 \int_0^l J_{M_i} \, dx \, dz = J_{M_i} l = u_i \tag{43}$$

Therefore a method to achieve equivalence to (15) is found as (33) can now be written in the MEC parameters as,

$$R \cdot \phi = F_{12} \tag{44}$$

3.2.4 Usages

Focusing on the broader picture of the design process, the above work shows that the more general FEM can be reduced to the MEC given specific design knowledge of the fields. Adding in that many including Hammond and Sykulski have shown how to relate permeance, a MEC parameter, to inductance, an EEC parameter, these analyses should be viewed less as discrete methods and more as a spectrum, which provides variable levels of detail. Understanding the spectrum of analyses can help a designer visualize how to sacrifice computational speed for accuracy and vice versa, as well as giving a more concrete meaning to the shift of modeling methods needed during the design process.

One such approach is the use of FEM to tune an EEC of an electric machine [64]-[69]. As previously mentioned, FEM models can be computationally expensive, but can take into account a number of phenomena that EEC do not. The tuning idea uses an FEM field solution to calculate the EEC lumped parameters, thus effects such as iron saturation are more or less accounted for in later EEC calculations. The advantage of which is evident when a designer needs to evaluate the performance of the electric machine with respect to other connected components.

For example Dyck et al. [64] looked at a FEM model of an induction motor driven by a PWM bridge electric circuit. The high switching frequency of the PWM necessitated a very small time step to be used when evaluating the coupled model, so much so that calculating that many FEM solutions was cost prohibitive. The authors instead proposed to “decouple” the PWM model directly from the field model by substituting an EEC induction motor model, allowing for computationally quick analysis even using the needed small time steps. The decoupling is accomplished by introducing an intermediate step where an FEM field solution is used to calculate the lumped parameter values of the EEC model from the proposed induction motor geometry. A fine example of selecting the right computational tools for the problem at hand.

3.3 Examples of early stage current induction motor design procedure

While all these FEM-involved methods are revolutionary in their own right. The true difficulty in design of electric machines is that all the methods presented solve the problem where knowledge is plentiful and solutions are scare, the opposite situation that a designer faces. The norm for routine design is that the solution is generally well known, for example a designer's known parameters might be the amount of startup torque, maximum rotational velocity, and the type of electrical feed available. The knowns tell the designer nothing about the geometry or size of the design being searched for. Additionally, high-level methods like the FEM provide field results, which do not provide any direct relations to machine parameters, for example decrease the airgap to increase torque.

The difficulties in such inverse-type processes were solved early on by making a number of assumptions based upon the knowns and parameters sought, applying these assumptions to analytical results, as well as applying empirical knowledge or previous design experiences. The traditional design process or at least the beginning of the process remained more or less unchanged since the early 1900s as evidenced by design calculation examples in books by Hird, 1908 [70]; Hamdi, 1994 [74]; and Boldea and Nasar, 2002 [6].

3.3.1 Historical 1908 example

Hird begins by proposing a design for a three-phase motor, that produces 100 horsepower at "500 revolutions per minute on a circuit of 500 volts and 25 periods" [70, pp. 228]. First Hird converts horsepower to watts, assumes an efficiency of 90%, and a power factor of 0.92. Using this information he calculates the volt-amperes each phase must carry and discusses the voltage and current trade-offs between star or delta winding connections. "The number of poles is fixed by the speed and periodicity, … the number of poles must be 6" [70, pp. 228]. Using a graph which relates the "output coefficient", the total volt-amperes over the feed voltage, to a coefficient representing the diameter squared times the length of the rotor core, "d^2l", Hird is able to choose a diameter and length that satisfy the coefficient relation. At this point the initial design sizing is roughly complete and the now antique circle diagram is utilized to calculate performance.

3.3.2 Modern 1994 example

Fast forwarding 86 years to Hamdi's design example, he begins by giving his knowns, "0.25 kW, 1380 rev/min, 415 V, star connected, 50 Hz, three-phase, 4-pole, squirrel-cage induction motor" [74, pp. 139]. In nearly the identical first step, Hamdi assumes an efficiency of 70% and a power factor of 0.70, and calculates a volt-amperes loading. Hamdi deviates from Hird and uses a different formula for calculating his "output coefficient", though the coefficient is calculated for the same reason, finding the product "D^2L". A diameter and length are chosen and further analysis is completed using slightly more modern techniques, including, of course, the Steinmetz equivalent circuit.

3.3.3 Modern 2002 example

Boldea and Nasar make reference to this design method in their example as well stating, "here we are going to use the widely accepted D_{is}^2L output constant concept..." [6, pp. 512]. The popularity of relating what is essentially a rotor volume measurement, D^2L, to an output coefficient is heavily grounded in how much energy can be sustained in that volume. The physics of the situation provide the upper bound based upon maximum field strengths and heat dissipation, eg how much flux can iron carry before it saturates and can the energy lost as heat in the motor be dissipated before the copper melts. The relationship of D^2L to the output coefficient has changed as materials and cooling methods have advanced, but the underlying physics have not. It is interesting to note that relating the rotor volume to the power output was recognized so early on in motor design history and remains the lowest common denominator today. Unfortunately one assumes the relationship to be highly empirical and most likely based upon a designer's previous designs, as Boldea and Nasar's begin their chapter on induction motor design by stating , "For the most part, [induction motor] design methodologies are proprietary" [6, pp. 509].

3.4 Tellegen's theorem for the magnetic equivalent circuit

Given the methods and examples thus far, the modern designer seems to be faced with starting the design process using the D^2L sizing concept, blindly guessing geometries to calculate field solutions using FEM, or using prior motor designs as briefly discussed in the introduction. One tool that seems absent is the use of sensitivity analysis to help better understand how input geometries relate to output parameters. Tellegen's theorem is commonly used in other fields, such as electric circuit design, however it appears to have been applied quite sparingly in the motor design area.

Tellegen's theorem is a fundamental theorem of network theory, which relies only upon KCL and KVL. Its lack of assumptions [71, pp. 2] make it nearly universally applicable; nonlinear, time-varying, or any number of complications present no issues given its generality. Literature in the field more or less starts with a reference to Tellegen's original paper in 1952 or the gold standard reference by Penfield et al. [71] published in 1970. The research community has used Tellegen in a number of ways, for example Dyck et al. [73] derives Tellegen's theorem for electromagnetic fields and applies it in order to image a hole in an aluminum block.

Utilizing a field-based version of Tellegen's theorem in the motor design case may be seen as non-ideal since a more computationally expensive method such as the FEM will be needed to solve the field problem. The situation will undoubtedly arise where a designer needs to evaluate more FEM solutions than is feasible. The MEC presents a strong case because it satisfies KCL and KVL, as shown above; it is easy to parameterize because it is lacks a rigidity in the way geometry is represented as real devices; and it is a relatively reduced-order model making it more suitable for quick repeated calculations for maximum responsiveness from the designer's perspective. To the best of the writer's knowledge, Tellegen's theorem has not been applied to the MEC before.

3.4.1 Derivation of Tellegen for magnetic equivalent circuit

The following derivation roughly follows the steps set out by Penfield et al. [71, ch. 2, pp. 4-22] with adaptations to the MEC parameters. Consider a network having no ports, made of branches, nodes, and parts. Applying KCL, where C is a sort of connection matrix that describes the connections between the branches, nodes, and parts; Φ is the independent flux with the subscript β denoting the branch through which the independent flux flows; taking all the independent fluxes together gives the net flux, ϕ, which is given with subscript α denoting the branch through which the net flux flows.

$$\phi_\alpha = \sum_\beta C_{\beta\alpha} \Phi_\beta \tag{45}$$

Similarly for KVL, where F_α is the MMF across each branch α.

$$\sum_\alpha C_{\beta\alpha} F_\alpha = 0 \tag{46}$$

Multiplying (45) by F_α

$$\phi_\alpha F_\alpha = \sum_\beta C_{\beta\alpha} \Phi_\beta F_\alpha = \sum_\beta \Phi_\beta C_{\beta\alpha} F_\alpha \tag{47}$$

Taking the sum of (47) over α

$$\sum_\alpha \phi_\alpha F_\alpha = \sum_\beta \Phi_\beta \left(\sum_\alpha C_{\beta\alpha} F_\alpha \right) \tag{48}$$

Applying (46) to (48) yields

$$\sum_\alpha \phi_\alpha F_\alpha = 0 \tag{49}$$

Since the MEC circuit topology does not change, previously calculated models can provide new information to revised designs. Cohn's theorem does just that, by estimating the change or sensitivity of a one-port network based upon the changes in variable elements that make up the network. Independently proved by many as early as the late-1920s and subject to a litany of generalizations and alternative derivations [71, pp. 79-80], Cohn's theorem is a basic result of one of the many ways Tellgen's theorem can be applied in the analysis of sensitivity.

Penfield et al. present their derivation of Cohn's theorem [71, pp. 79-80] in terms of electrical impedances and parameters. As shown with Tellegen above, a similar derivation can be done for MEC elements and parameters, however a few generalizations of (49) are needed. Penfield et al. introduce the idea of a Kirchhoff operator [71, pp. 14-

15], which “are defined as those which yield, from a set of currents (voltages) that obey Kirchhoff's current (voltage) law, a set of numbers or functions that also obey Kirchhoff's current (voltage) law” [71, pp. 113-115], i.e. if some operation or transformation is done to the system which obeys KCL and KVL, the transformed system still obeys KCL and KVL. Such constraints allow for Tellegen to be applied to both the pre- and post-operated upon system as well as the pre- and post-operated upon system which shares the same network topology. A general form [71, pp. 14-15] of Tellegen's theorem can be expressed as

$$\sum_{p} \Lambda' \phi_p \, \Lambda'' F_p = \sum_{\alpha} \Lambda' \phi_\alpha \, \Lambda'' F_\alpha \tag{50}$$

Where Λ is the arbitrary Kirchhoff operator and the prime denotes that two different operators can be applied [71, pp. 14-15]. To get to Cohn's theorem, Penfield et al. applies Tellegen to a “one-port network with port” reluctance R, “made of two-terminal elements with” reluctances R_α [71, pp. 79-80]. The latter condition is satisfied by definition in the MEC since reluctances are only two terminal elements. Since each small change in a reluctance element, δR_α, causes a corresponding change in flux and MMF distributions in the network, the overall reluctance changes by a small amount as well, δR.

Consider a combination of (11) and (18),

$$\phi^2 \cdot \delta R = \phi \cdot \delta(R\phi) - \delta\phi \cdot R\phi = \phi \cdot \delta F - \delta\phi \cdot F \tag{51}$$

Where center dots have been added above to highlight which variable the δ, a small change, is operating on.

Using the general form of Tellegen's above, interchanging the Kirchhoff operators and subtracting the equation from itself, gives the difference form of Tellgen's theorem

$$\sum_{p} \left(\Lambda' \phi_p \Lambda'' F_p - \Lambda'' \phi_p \Lambda' F_p \right) = \sum_{\alpha} \left(\Lambda' \phi_\alpha \Lambda'' F_\alpha - \Lambda'' \phi_\alpha \Lambda' F_\alpha \right) \tag{52}$$

Applying the difference form to (52), selecting Λ' to be the Fourier transform, Λ'' to be "the small changes" [71, pp. 79-80], and taking the sum over p yields

$$\phi \cdot \delta F - \delta\phi \cdot F = \sum_{\alpha} \left(\phi_\alpha \cdot \delta F_\alpha - \delta\phi_\alpha \cdot F_\alpha \right) \tag{53}$$

Since (51) holds for each branch it can be applied to simplify (53), thus Cohn's theorem for the MEC is found

$$\phi^2 \cdot \delta R = \sum_{\alpha} \phi_\alpha^2 \cdot \delta R_\alpha \tag{54}$$

The result allows for a small change in R to be related back to a small change in the overall reluctance of the system knowing only the fluxes at each branch α and the overall flux at the port. Similarly a Cohn's theorem using MMF and permeance can be found using the same steps

$$F^2 \cdot \delta P = \sum_{\alpha} F_\alpha^2 \cdot \delta P_\alpha \tag{55}$$

3.4.2 An example application

An interesting result is the similarity of Cohn's theorem to the torque equation derived by Ostović [47, pp. 75-85],

$$T = T_{loss} + J \frac{d^2\gamma}{dt^2} + \sum_{pn} F_j^2 \frac{dP_j}{d\gamma} \tag{56}$$

Where T is the torque, T_{loss} is the torque lost to purely mechanical losses, J is the total inertia on the shaft, γ is the angle of rotation, P_j is the permeance at the j-th node, and the sum over pn denotes only the elements that are parametrically nonlinear. In the case of the induction motor, parametrically nonlinear elements are relegated to the air gap, where their nonlinearity arises from changing geometries as the rotor angle, γ, is swept.

Therefore in the MEC, Cohn's theorem can also be seen in some instances to be the sensitivity of the torque, since a small change in gamma causes a small change in the permanences of the elements in the air gap. There are many other applications to be explored, one for example would be using the above results to look at changes in stator windings specifically the change in the number of turns around a tooth or teeth. Combining (51) with (55) and acknowledging that the left-hand side of (55) represents a the change in torque yields,

$$\delta T = \sum_{\alpha} \left(\phi_\alpha \cdot \delta F_\alpha - \delta \phi_\alpha \cdot F_\alpha \right) \tag{57}$$

Summing over all the branches is unnecessary if the small change is due to the stator windings, since only the stator teeth branches will have nonzero contributions. The MMF and flux in the stator teeth have a special relation to the electrical input to the system through flux linkages. Ostović expresses this relationship through a very extensive system of matrices to mathematically model the different winding types found in real devices [47, ch. 3, pp. 140-189]. For a single-layer winding Ostović gives the following formula [47, pp. 168] for the stator teeth MMF, F_{st}, due to the electric current, i,

$$F_{st} = w'' \, i \tag{58}$$

Where w'' is defined as the MMF transform matrix. If the sum is only over the stator teeth, then adopting the element and node names from Appendix A and applying to (57) gives,

$$\delta T_{st} = \sum_{j}^{all\ st} \phi_{st,j} \cdot \delta F_{12} - \delta \phi_{st,j} \cdot F_{12} \tag{59}$$

Where st denotes stator tooth.

From (4) and (11),

$$F_{12} = u_{2,j} - u_{1,j} + F_{st,j} \tag{60}$$

$$\phi_{st,j} = \left(u_{2,j} - u_{1,j} \right) P_{st,j} \tag{61}$$

Substituting (60) and (61) into (59) gives,

$$\delta T_{st} = \sum_{j}^{all\ st} \phi_{st,j} \cdot \delta\left(u_{2,j} - u_{1,j} + F_{st,j}\right) - \delta\left(P_{st,j}\left(u_{2,j} - u_{1,j}\right)\right)\left(u_{2,j} - u_{1,j} + F_{st,j}\right) \tag{62}$$

Assuming there is no small change in the potential at u_1 or u_2 and substituting (58) for F_{st},

$$\delta T_{st} = \sum_{j}^{all\ st} \phi_{st,j} \cdot \delta\left(w'' \, i\right) \tag{63}$$

Ostović breaks w'' down into a number of matrices which describe the winding topology [47, pp. 167],

$$w'' = \boldsymbol{M}_{tmmf}^{-1} \, \boldsymbol{I}'_{k,k} \, \boldsymbol{M}_{sat} \, \boldsymbol{M}_{tc} \, \boldsymbol{M}_{cc} \, i \tag{64}$$

Where M_{tmff}, the tooth MMF matrix, defines the relationship between slot ampere-turns and tooth MMF; I' is the incomplete identity matrix [47, pp. 331, eqn. A.I.8]; M_{sat}, the slot ampere-turns matrix, translates between ampere-turns in slots and coil ampere-turns; M_{tc}, the turns per coil matrix, contains only diagonal entires of the number of turns for each coil; and M_{cc}, the coil currents matrix, which equates phase currents with coil currents [47, pp. 167-169]. The only matrix for which the small change will be applied is M_{tc}, the turns per coil matrix. Thus the sensitivity of the torque to small changes in the number of stator windings is,

$$\delta T_{st} = \sum_{j}^{all\ st} \phi_{st,j} \cdot \left(\boldsymbol{M}_{tmmf}^{-1} \, \boldsymbol{I}'_{k,k} \, \boldsymbol{M}_{sat} \, \delta \boldsymbol{M}_{tc} \, \boldsymbol{M}_{cc} \, i\right)_j \tag{65}$$

Even though no notation has been given it is noted that *i* is a vector and *M*'s and *I* are matrices, matrix vector multiplication rules apply.

Sensitivity analysis with Tellegen's theorem can provide helpful direction to a designer as a design is iteratively tweaked and moved closer to the final design specifications. The analysis can also be helpful at the end of the design process if a designer needs to, for example, evaluate how changes due to manufacturing tolerances will affect performance bounds. The first-order [71, pp. 79-80] analysis is also computationally inexpensive since the only information needed beyond the MEC topology used is a current solution. Further study is needed to refine and quantify the accuracy and computational efficiency of these methods. Other's including Amrhein have alluded to the advantageous “parameterization” [38, pp. 27] capabilities of the MEC, perhaps applying Tellegen is the unexplored secret.

CHAPTER 4
Conclusion

In the last few decades, the world of electric machine design, specifically induction machine design, has been reinvigorated by the introduction of power electronics. Where designers were once limited to a single alternating current waveform with constant voltage and frequency, power electronics have thrown all those assumptions out the window. The change has necessitated new design methods that go beyond the typical induction motor EEC seen in every textbook for the last century and have sent designers back to first principles.

The engineering design process for electric machines is undoubtedly a nontrivial task. A designer usually sets off with a rough idea about values of terminal parameters and overall dimensions, that provide at best a cursory summary of the machine and at worst describe one that is fictitious. At the beginning of the design process, the goal is to quickly narrow the design space, making sure rough machine parameters are satisfied and leaving the finer details of the design specifications for later. The CAD tools needed to assist the designer in this phase must perform quick calculations to maximize rough design iterations.

As the designer refines the coarse design and needs finer-grain control over how it is being modeled, the CAD tool is faced with the difficulty that its current analysis method is inadequate. The obvious choice is to move to another more complicated model.

However, moving from one analysis method to another creates problems of its own, such as when exactly to transition and how to integrate the knowledge from the previous stage. What is needed is a spectrum of analyses, rather than a discrete set of tools.

In the electric machines area, literature has mainly focused on three methods: the EEC, the MEC, and the FEM. The EEC has been in use for more than a century, simplicity and age notwithstanding, its empirically-tuned parameters continue to provide results for the majority of designs. Unlike the EEC, the FEM approaches analysis with no abstraction from the physics and is able to accurately incorporate as many phenomena as needed at the cost of complexity. The MEC straddles the area between EEC and FEM, its MMF and magnetic-flux formulation remain arguably truer to the underlying physics and allow it to model phenomena, such as iron saturation, more easily than the EEC. However, the MEC has seen markedly less research than the EEC and FEM even as some authors [38, pp. 99] make the case for an MEC-based CAD package.

The need for such a tool to bridge between the EEC and FEM is not an unreasonable request. The MEC undoubtedly provides an excellent compromise between the speed of the EEC and the customizable accuracy of the FEM. Its treatment of the physics at play leads to a reduced-order model that is full of ancillary benefits, such as being able to apply a circuit-based sensitivity analysis using Tellegen's theorem. The doubt arises because the creation of another design package may be a fruitless pursuit.

It has been shown above that the generality of the FEM can be used to create an MEC element, given suitable knowledge or assumptions. In the interest of creating a spectrum of analyses, rather than creating an entirely new design package centered on the MEC, why not augment the readily available, better documented, and already polished FEM tools with the MEC knowledge.

Appendix A

Fig. 4: A "simple" topology for an induction motor MEC, adapted from [47, pp. 99]

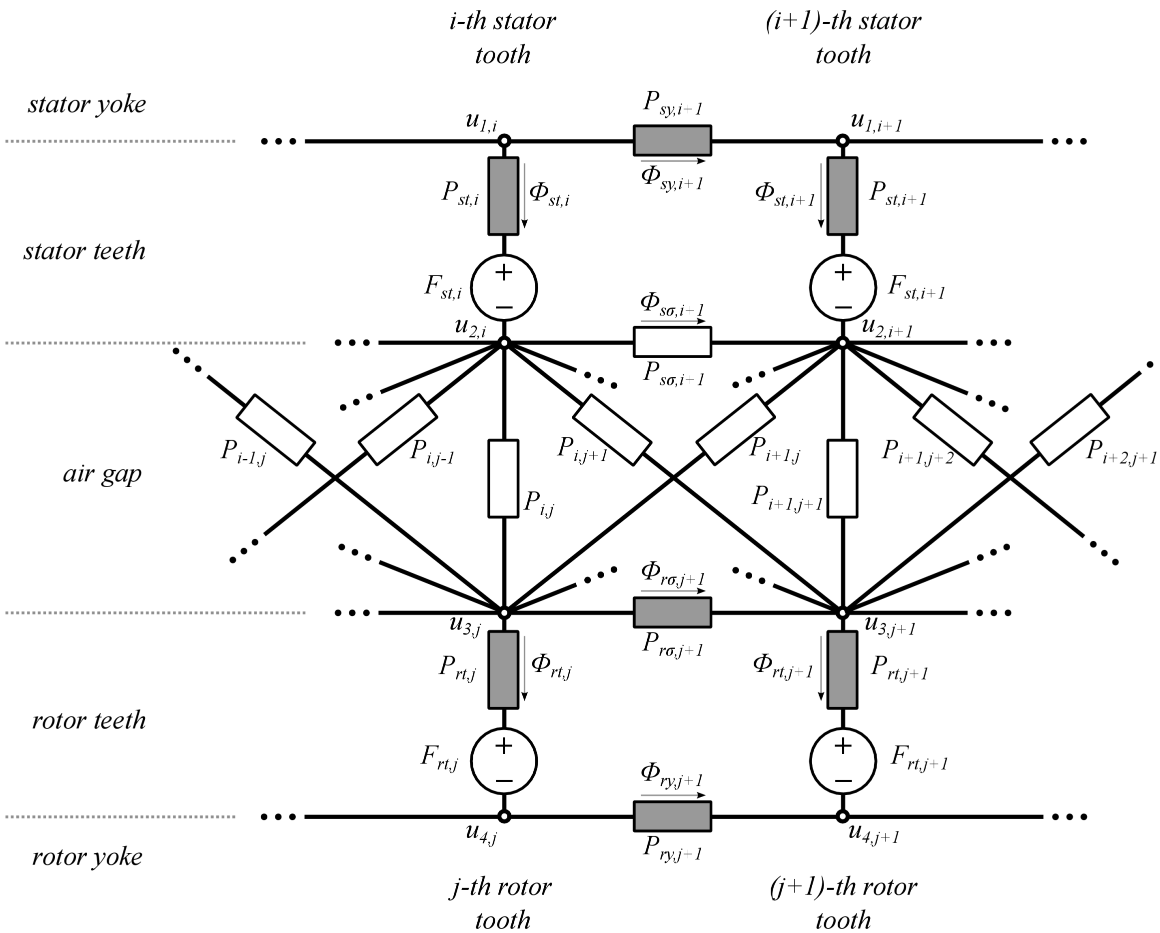

References

1 E. K. Antonsson, *Design Quotations* [Online]. Available: http://www.design.caltech.edu/erik/Misc/design_quotes.html

2 A. K. Goel, "Design, analogy, and creativity," *IEEE Expert*, vol. 12, pp. 62-70, 1997. doi: 10.1109/64.590078

3 D. C. Brown. *Routineness Revisited* [PDF]. Available: http://www.wpi.edu/academics/cs/~dcb/Papers/waldron-book.mkr.pdf

4 J. Ouyang, "Case-based reasoning for the creative design of electromagnetic devices," Ph.D. dissertation, Elect. and Comp. Eng., McGill Univ., Montreal, QC, 2012. Available: http://digitool.library.mcgill.ca/R/?func=dbin-jump-full&object_id=107659

5 D. Leake, *Case-based reasoning: Experiences, lessons and future directions*. Cambridge: MIT Press, 1996.

6 I. Boldea and S. A. Nasar, *The induction motor handbook*. Boca Raton: CRC Press, 2002.

7 R. Kline, "Science and engineering theory in the invention and development of the induction motor, 1880-1900." *Tech. and Culture*, vol. 28, no. 8, pp. 283-313, Apr. 1987. Available: http://www.jstor.org/stable/3105568

8 W. Bailey, "A mode of producing Arago's rotations," *Proc. Phys. Soc.*, vol. 3, no. 15, pp. 115-119, June 1879. Available: http://iopscience.iop.org/1478-7814/3/1/318

9 M. Deprez, "Sur le synchronisme électrique de deux mouvements relatifs, et de son application á la construction d'une nouvelle boussole électrique," *Comptes Rendus des Séances de L'Académie des Sciences*, vol. 97, pp. 1193-1195, 1883. Available: http://gallica.bnf.fr/ark:/12148/bpt6k3053w

10 S. P. Thompson, *Polyphase electric currents and alternate current motors*, London: Spon and Chamberlin, 1895. ark:/13960/t6348qr0b

11 S. P. Thompson, *Dynamo-electric machinery*, 4th ed. New York: Harvard Pub. Co., 1893. Available: http://catalog.hathitrust.org/api/volumes/oclc/67533864.html

12 S. P. Thompson, *Dynamo-electric machinery*, 2nd ed. London: E. & F. N. Spon, 1886. ark:/13960/t79s1mw8s

13 Muzej Nikole Tesle. (2008, Mar 27). *Nikola Tesla Museum* [website]. Available: http://tesla-museum.org/meni_en.htm

14 K. J. Dood et al., "Tesla and the induction motor," *Tech. and Culture*, vol. 30, no. 4, pp. 1013-1023, Oct., 1989. Available: http://www.jstor.org/stable/3106202

15 N. Tesla, "Electro-magnetic motor," U.S. Patent 381 968, May 1, 1888.

16 N. Tesla, “Electro-magnetic motor,” U.S. Patent 382 279, May 1, 1888.

17 T. P. Hughes, *Networks of power: electrification in Western society, 1880-1930*. Baltimore: Johns Hopkins Uni. Press, 1983. Available: http://hdl.handle.net.proxy2.library.mcgill.ca/2027/heb.00001.0001.001

18 G. Ferraris, “Rotazioni elettrodinamiche prodotte per mezzo di correnti alternate ,” *Il Nuovo Cimento Series 3* , vol. 23, no. 1, pp. 246-263, Dec. 1888. doi: 10.1007/BF02730244 Available: http://dx.doi.org/10.1007/BF02730244

19 G. Ferraris, “Electrodynamic rotations produced by means of alternate currents,” *The Electrician*, vol. 36, pp. 281-283, Dec. 1895. (Available in McGill Redpath Basement Storage: folio 22, 349)

20 M. von Dolivo-Dobrowolsky, “Alternating-current motor,” U.S. Patent 427 978, May 1890.

21 M. von Dolivo-Dobrowolsky, “Regulation of alternating-current motors,” U.S. Patent 503,038, Aug. 1893.

22 B. G. Lamme, “Story of the induction motor,” *J. of the Amer. Inst. of Elect. Eng.*, vol. 40, pp 203-223, Mar. 1921. Available: http://hdl.handle.net/2027/njp.32101048908923

23 P. L. Alger and R.E. Arnold, “The history of induction motors in America,” *Proc. of the IEEE*, vol. 64, no. 9, pp 1380-1383, Sept. 1976. doi: 10.1109/PROC.1976.10329

24 D. W. Jordan, “The magnetic circuit model, 1850-1890: the resisted flow image in magnetostatics,” *British J. for the History of Sci.*, vol 23. pp 131-173, 1990. doi: 10.1017/S0007087400044733

25 G. Kapp, “The pre-determination of the characteristics of dynamos,” *Telegraph-Engineers and Electricians, J. of the Soc. of*, vol 15. no. 64., pp 518-530, 1886. Available via Google Books.

26 J. N. Shoolbred et al., “Further discussion on: the pre-determination of the characteristics of dynamos,” *Telegraph-Engineers and Electricians, J. of the Soc. of*, vol 15. no. 64., pp 581-595, 1886. Available via Google Books.

27 B. A. Behrend, *The induction motor: A short treatise on its theory and design, with numerous experimental data and diagrams*. New York: Electrical world and engineer, 1901.

28 B. A. Behrend, *The induction motor and other alternating current motors: Their theory and principles of design*. New York: McGraw-Hill, 1921.

29 MagNet version 7, Montreal, Quebec: Infolytica Corporation, 2013. Available: http://www.infolytica.com/en/products/magnet/

30 Motorsolve, Montreal, Quebec: Infolytica Corporation, 2013. Available: http://www.infolytica.com/en/products/motorsolve/

31 SPEED, Ellesmere, Shropshire: Motor Design Ltd, 2013. Available: http://www.motor-

design.com/speed.php

32 RMxprt, Ansys Inc., 2013. Available: http://www.ansys.com/Products/Simulation+Technology/Electromagnetics/Electromechanical+Design/ANSYS+RMxprt

33 Maxwell, Ansys Inc., 2013. Available: http://www.ansys.com/Products/Simulation+Technology/Electromagnetics/Electromechanical+Design/ANSYS+Maxwell

34 M. V. K. Chari and P. P. Silvester, *Finite elements in electrical and magnetic field problems*. Chichester: Wiley, 1980.

35 R. Ferrari, “The Finite-Element Method, Part 2: P. P. Silvester, an Innovator in Electromagnetic Numerical Modeling,” *IEEE Antennas Propagat. Mag.*, vol. 49, pp. 216-234, June, 2007. (specifically pp. 7-9) doi: 10.1109/MAP.2007.4293978

36 P.P. Silvester and R. L. Ferrari, *Finite Elements for Electrical Engineers*, 1st ed. Cambridge: Cambridge University Press, 1983.

37 S. J. Salon, *Finite Elements Analysis of Electrical Machines.* Boston: Kluwer Academic Publishers, 1995.

38 M. Amrhein, “Induction machine performance improvements – design-oriented approaches,” Ph.D. dissertation, Elect. and Comp. Eng., Univ. of Illinois at Urbana-Champaign, Urbana, IL, 2007. Available: http://search.proquest.com/docview/304854534

39 E. R. Laithwaite. “Magnetic equivalent circuits for electric machines,” *Proc. IEE*, vol. 114, pp. 1805-1809, Nov. 1967. doi: 10.1049/piee.1967.0344

40 C.J. Carpenter, "Magnetic equivalent circuits," *Proc. IEE*, vol. 115, no. 10, pp. 1503-1511, October 1968. doi: 10.1049/piee.1968.0265

41 V. Ostović, “Analiza prijelaznih pojava u zasićenim električnim strojevima primjenom magnetskih ekvivalentnih shema,” Ph.D. dissertation, University of Zagreb, 1982 .

42 V. Ostović, “A Method for Evaluation of Transient and Steady State Performance in Saturated Squirrel Cage Induction Machines,”*IEEE Trans. Energy Convers.* , vol. EC-l, no. 3, pp. 190-197 , Sept. , 1986. doi: 10.1109/TEC.1986.4765754

43 V. Ostović, “Computation of Saturated Permanent Magnet A.C. Motor Performance by Means of Magnetic Circuits,” *IEEE Trans. Ind. App.*, vol. IA-23, pp. 836-841, Sept./Oct., 1987. doi: 10.1109/TIA.1987.4504992

44 V. Ostović, “A Simplified Approach to the Magnetic Equivalent Circuit Modeling of Electric Machines,” *IEEE Trans. Ind. App.*, vol. 24, pp. 308-316, Mar./Apr., 1988. doi: 10.1109/28.2871

45 V. Ostović, “Magnetic Equivalent Circuit Presentation of Electric Machines,” *Electric Machines and Power Systems*, vol. 12, no. 6, pp. 407-432, June, 1987. doi: 10.1080/07313568708960120

46 V. Ostović, “A Novel Method for Evaluation of Transient States in Saturated Electric Machines,” *IEEE Trans. Ind. App.*, vol. 25, pp. 96-100, Jan./Feb., 1989. doi: 10.1109/28.18874

47 V. Ostović, *Dynamics of Saturated Electric Machines*. New York: Springer-Verlag, 1989.

48 P. Sewall et al., “Efficient dynamic models for induction machines,” *Intl. J. Numerical Modeling*, vol. 12, pp. 449-464, 1999. doi: 10.1002/(SICI)1099-1204(199911/12)12:6<449::AID-JNM365>3.0.CO;2-W

49 J. Perho, “Reluctance network for analysing induction machines,” D.Sci thesis, Dept of Elect. and Commun. Eng., Helsinki Univ. of Tech., Helsinki , Finland, 2002. Available http://lib.tkk.fi/Diss/2002/isbn9512260905/isbn9512260905.pdf

50 S. D. Sudhoff et al., “Magnetic Equivalent Circuit Modeling of Induction Motors,” *IEEE Trans. Energy Convers.*, vol. 22, pp. 259-270, June, 2007. doi: 10.1109/TEC.2006.875471

51 M. Bash et al., “Incorporating Motion in Mesh-Based Magnetic Equivalent Circuits,” *IEEE Trans. Energy Convers.*, vol. 25, pp. 329-338, June, 2010. doi: 10.1109/TEC.2009.2035513

52 H. W. Derbas, “A Comparison of Nodal- and Mesh-Based Magnetic Equivalent Circuit Models,” *IEEE Trans. Energy Convers.*, vol. 24, pp. 388-396, June, 2009. doi: 10.1109/TEC.2008.2002037

53 M. Yilmaz and P. T. Krein, “Capabilities of Finite Element Analysis and Magnetic Equivalent Circuits for Electrical Machine Analysis and Design,” in *Proc. IEEE Power Electronics Specialists Conf.*, Rhodes, Greece, 2008, pp. 4027-4033. doi: 10.1109/PESC.2008.4592584

54 Gyselinck et al., “Hybrid magnetic equivalent circuit – finite element modelling of transformer fed electrical machines,” *COMPEL*, vol. 22, no. 3, pp. 643-658, 2008. doi: 10.1108/03321640310475092

55 P. Dular et al., “Dual Finite Element Formulations for Lumped Reluctances Coupling,” *IEEE Trans. Magn.*, vol. 41, pp 1396-1399, May, 2005. doi: 10.1109/TMAG.2005.844348

56 D. A. Philips, “Coupling Finite Elements and Magnetic Networks in Magnetostatics,” *Intl J. Numerical Methods Eng.*, vol. 35, pp. 1991-2002, 1992. doi: 10.1002/nme.1620351005

57 P. Dular et al., “Perturbation finite-element method for magnetic circuits ,” *IET Sci. Meas. Technol .*, vol. 2, no. 6, pp. 440-446, 2008. doi: 10.1049/iet-smt:20080092

58 Y. D. Chun et al., “Comparison between three-dimensional (3D) equivalent magnetic circuit network method and 3D finite element method for magnetic-field computation ,” *J. of Applied Physics*, vol. 97, no. 10E105, 2005. doi: 10.1063/1.1853195

59 P. Hammond and J. K. Sykulski, *Engineering electromagnetism: physical processes and computation.* New York: Oxford Univ. Press, 1994.

60 P. Hammond and D. Baldomir, “Dual energy methods in electromagnetism using tubes and slices,” *IEE Proc.*, vol. 135, pt. A, no. 3, pp. 167-172, March, 1988.

61 P. Hammond and J. Sykulski, "Tubes and Slices: A New Way of Teaching the Principles of Electric and Magnetic Field," *IEEE Trans Edu.*, vol. 35, pp. 300-306, November, 1992. doi: 10.1109/13.168704

62 Weiss et al., "Finite Element Analysis of Magnetic Fields with Permanent Magnet," *IEEE Trans. Magn.*, vol. 20, pp. 1933-1935, Sept., 1984. doi: 10.1109/TMAG.1984.1063462

63 J. Jin, *The Finite Element Method in Electromagnetics*, 2nd ed. New York: Wiley, 2002.

64 D. N. Dyck et al., "A Performance Model of an Induction Motor for Transient Simulation With a PWM Drive," *IEEE Trans Magn.*, vol. 46, pp. 3093-3096, August 2010. doi: 10.1109/TMAG.2010.2043652

65 K. Yamazaki, "An Efficient Procedure to Calculate Equivalent Circuit Parameter of Induction Motor Using 3-D Nonlinear Time-Stepping Finite-Element Method ," *IEEE Trans. Magn.*, vol. 38, pp. 1281- 1284, March, 2002. doi: 10.1109/20.996327

66 D. Dolinar et al., "Calculation of two-axis induction motor model parameters using finite elements," *IEEE Trans. Energy Convers.*, vol. 12, pp. 133-142, June, 1997. doi: 10.1109/60.629695

67 S. Williamson and M. J. Robinson, "Calculation of cage induction motor equivalent circuit parameters using finite elements," *IEE Proc. B,* vol. 138, no. 5, pp. 264-276, Sept., 1991.

68 M. H. Gmiden and H. Trabelsi, "Calculation of Two-Axis Induction Motor Model using Finite Elements with Coupled Circuit ," in *2009 6th Int. Multi-Conf. Systems, Signals and Devices*, 2009. doi: 10.1109/SSD.2009.4956785

69 R. Prieto et al., "Bridging the Gap Between FEA Field Solution and the Magnetic Component Model," in *12th Annu. IEEE Applied Power Electronics Conf. And Expo.*, Austin, TX, vol. 2, pp. 1315-1321, 2005. doi: 10.1109/APEC.2005.1453177

70 W. B. Hird, *Elementary dynamo design, with numerical examples*. London: Cassell and Company, Limited, 1908.

71 P. Penfield et al., *Tellegen's theorem and electrical networks*. Cambridge: MIT Press, 1970.

72 C. P. Steinmetz, "The alternating current induction motor," *Trans. Amer. Inst. Elect. Engineers*, vol. XIV, pp. 183-217, Jan., 1897. doi: 10.1109/T-AIEE.1897.5570186

73 D. N. Dyck et al., "A method of computing the sensitivity of electromagnetic quantities to changes in materials and sources," *IEEE Trans. Magn.*, vol. 30, pp. 3415-3418, Sept., 1994. doi: 10.1109/20.312672

74 E. S. Hamdi, *Design of small electric machines*. New York: Wiley, 1994.